ORIGINAL ARTICLE

Stereotactic Administration of Edaravone Ameliorates Collagenase-Induced Intracerebral Hemorrhage in Rat

Yan Zhang,[1,2,3] Yang Yang,[2] Guang-Zhu Zhang,[2] Mou Gao,[2] Guang-Zhi Ge,[2] Qin-Qin Wang,[2] Xin-Chao Ji,[2] Yi-Lin Sun,[4] Hong-Tian Zhang[2,3] & Ru-Xiang Xu[2,3]

1 The Third Military Medical University, Chongqing, China
2 Affiliated Bayi Brain Hospital, Army General Hospital of PLA, Beijing, China
3 The Neurosurgical Research Center of Beijing Military Region, Beijing, China
4 Department of Ultrapathology of Beijing Neurosurgical Institute, Beijing, China

Correspondence

Prof. Ru-Xiang Xu, Affiliated Bayi Brain Hospital, Army General Hospital of PLA, The Neurosurgical Research Center of Beijing Military Region, NO.5, Nanmencang, Dongsishitiao Street, Dongcheng District, Beijing 100700, China.
Tel.: +86-10-64021575;
Fax: +86-10-66399833;
E-mail: brain_xu@126.com
and
Dr. Hong-Tian Zhang, Affiliated Bayi Brain Hospital, Army General Hospital of PLA, The Neurosurgical Research Center of Beijing Military Region, NO.5, Nanmencang, Dongsishitiao Street, Dongcheng District, Beijing 100700, China.
Tel.: +86-10-66721204;
Fax: +86-10-66399833;
E-mail: zhanghongtian2016@126.com

SUMMARY

Background: Edaravone is widely used for treating ischemic stroke, but it is not still confirmed in intracerebral hemorrhage (ICH) as an ideal medication targeting the brain parenchyma. We aimed to investigate the neuroprotective effects of stereotactic administration of edaravone (SI) into the brain parenchyma. **Methods:** Intracerebral hemorrhage rat models were established by infusion of collagenase into the caudate nucleus. Neural functional recovery was assessed using modified neurological severity scores (mNSS). A comparative study of therapeutic effects between SI and intraperitoneal injection of edaravone (IP) involved in cerebral edema, blood–brain barrier (BBB) permeability, hematoma absorption, inflammatory response and neuronal apoptosis. **Results:** Compared with IP, the mNSS was significantly ($P < 0.05$) improved by SI; cerebral edema and BBB permeability were dramatically ameliorated ($P < 0.05$); IL-4 and IL-10 levels increased, but IL-1β and TNF-α levels significantly decreased; neuron apoptosis decreased markedly ($P < 0.05$); and caspase-3 and Bax expression significantly dropped, but Bcl-2 increased in SI group ($P < 0.05$). **Conclusion:** SI markedly improved neurological deficits in ICH rat models via antiinflammatory and antiapoptosis mechanisms and promoted M2-type microglia differentiation. SI was effective in rats with collagenase-induced ICH.

The first two authors contribute equally to this work.

Introduction

Intracerebral hemorrhage (ICH) accounts for 20–30% of all strokes in China, with a mortality rate of 30–40% during the acute phase and a recurrence rate of 1.8–11% [1]. Hematoma during early ICH can directly compress brain tissue, which further leads to mechanical injury and additional secondary brain injury, as well as excitotoxic-related neurological deterioration [2], inflammatory responses and neuronal cell death [3]. Controversy remains regarding surgical procedures and conservative treatment paradigms with respect to clinical outcome and mortality rate [4]. Edaravone, an effective free radical scavenger and antioxidant, can alleviate cerebral edema [5], and in the clinic, it has been widely used for treating ischemic stroke. However, few literature

has reported the effectiveness of edaravone in treating ICH. As intravenous administration is still routinely used for edaravone administration, few studies have analyzed the effects of the direct intracranial route. Along with advances in stereotactic and image-guided technology, the safety of intracranial stereotactic injection has dramatically improved. Additionally, stereotactic delivery is the most important mean for the minimally invasive clinical treatment of ICH [6]. Following invasive surgery, edaravone can be subsequently injected into the damage zone of hematoma. The current study established rat models of ICH by collagenase type VII and then compared the treatment efficacy of stereotactic and intraperitoneal delivery of edaravone. Additionally, we attempted to identify the action mechanisms of edaravone.

Materials and Methods

Experimental Design and Groups

Healthy, adult, male, Sprague Dawley (SD) rats (Vital River Laboratory Animal Technology, Beijing, China) weighing 250–280 g were housed at 25°C and 40–60% humidity with lights on from 8:00 to 22:00. The rats had free access to food and water. Experimental protocols were approved by the Ethics Committee for Animal Experimentation of General Hospital of Beijing Military Region, PLA (approved number: 2015–129). Utmost efforts were made to minimize the number of animals for experiments. The experiment paradigm is shown in Figure 1A. With limits of the Ethics Committee for Animal Experimentation and researches reported previously [7–9] considered comprehensively, 201 rats were selected finally and randomly divided into the following four groups (3–6 rats in each assay): (1) sham treatment (sham, n = 15), incisions were made in the scalp to expose the skull and burr holes were drilled and punctured by the needle without injecting collagenase; (2) saline control (saline, n = 50), rats were stereotactically injected with 10 μL saline into the hematoma cavity at 24 and 72 h post-ICH; (3) intraperitoneal (i.p.) injection of edaravone (IP, n = 68), rats were intraperitoneally injected with 3 mg edaravone/kg body weight (Nanjing Simcere, Nanjing, China, specifications 20 mL: 30 mg) at 1, 24, 48, and 72 h post-ICH; and (4) stereotactic injection of edaravone (SI, n = 68), 10 μL edaravone of 1.5 mg/mL was microinfused stereotactically into the hematoma cavity at 24 and 72 h post-ICH.

ICH Models

Sprague Dawley rats were anesthetized with 3.6% chloral hydrate (10 mL/kg, i.p.; Sigma-Aldrich, St. Louis, MO, USA) following 12-h fasting and 4-h water deprivation. ICH was induced by stereotactically infusing collagenase VII (0.4 U in 0.8 μL sterile saline, C0773; Sigma-Aldrich) into the caudate nucleus. The injection coordinates were 3.0 mm right, 0.5 mm anterior, and 5.5 mm ventral from bregma at the skull surface using a stereotactic instrument (Stoelting, Wood Dale, IL, USA). Collagenase was continuously injected for 4 min at a speed of 200 nL/min. The needle was then held in place for another 10 min to prevent backflow, and the hole was sealed with bone wax. The rats were then housed in a biologically clean room. Neurological abnormalities were assessed according to a modified neurological severity scores (mNSS), and scores were recorded at 0.5, 1.5, 3, 7, 14, and 28 days post-ICH by two independent investigators blinded to the experimental treatment scheme. Neurological function was graded on a scale of 0–18 (normal score, 0; maximal deficit score, 18) [10].

Whole-Brain MRI Scan

To measure hematoma volumes, rats were randomly selected at days 2, 14, and 28 post-ICH. We performed whole-brain MRI scan using a 7.0-Tesla MRI scanner (Bioclinscan, Bruker, Germany); T2 times were used to observe blood volume, and ipsilateral ventricular volume was used to evaluate brain tissue lesion. The image acquisition parameters were as follows: TR: 3140 ms, TE: 37 ms, the field of view (FOV): 40 × 40 mm, flip angle: 180. All results were reported using the software 3D slicer 4.4.0 (64 bit, The Brigham and Women's Hospital Inc., Boston, MA, USA).

Evaluation of Brain Edema

Brain tissue was weighed to obtain immediate wet weight. The tissue was then dried at 100°C for 48 h to obtain dry weight. The water content of brain tissue = [(wet weight) – (dry weight)]/(wet weight) × 100%.

Brain Section and Histopathology

We performed the methods according to a previous study [11]. Following deep anesthesia with pentobarbital, the rats were transcardially perfused with 0.9% saline and then 4% paraformaldehyde in 0.1 M phosphate-buffered saline (PBS, pH 7.4); 12-μm sections were mounted on glass slides for hematoxylin and eosin (H&E) stainings, other histological stainings, and immunofluorescence. All materials for staining were sampled from the brain tissue around the focus of cerebral hemorrhage. Image analysis was performed by the Image-Pro Plus 6.0 (Media Cybernetics Inc., Rockville, MD, USA).

Evaluation of Blood–Brain Barrier (BBB) Disruption

Rats were selected randomly to assess the vascular permeability of BBB by Evans blue and transmission electron microscope (TEM) assays, which were performed as reported previously [12].

Luxol Fast Blue Staining for Myelin Damage

The tissue sections were soaked in 95% ethanol for 2 min and subsequently in Luxol Fast Blue solution (S3382; Sigma) at 56°C overnight. For image analysis, the ratio of the area in the damaged side to the area in the normal side represented the degree of myelin injury.

Immunofluorescence and Apoptosis Assays

Standard protocols were performed on 12-μm-thick sections using the following primary antibodies: NF200 (Cat#.ab82259, Abcam, Cambridge, UK) for neurofilament protein; glial fibrillary acidic
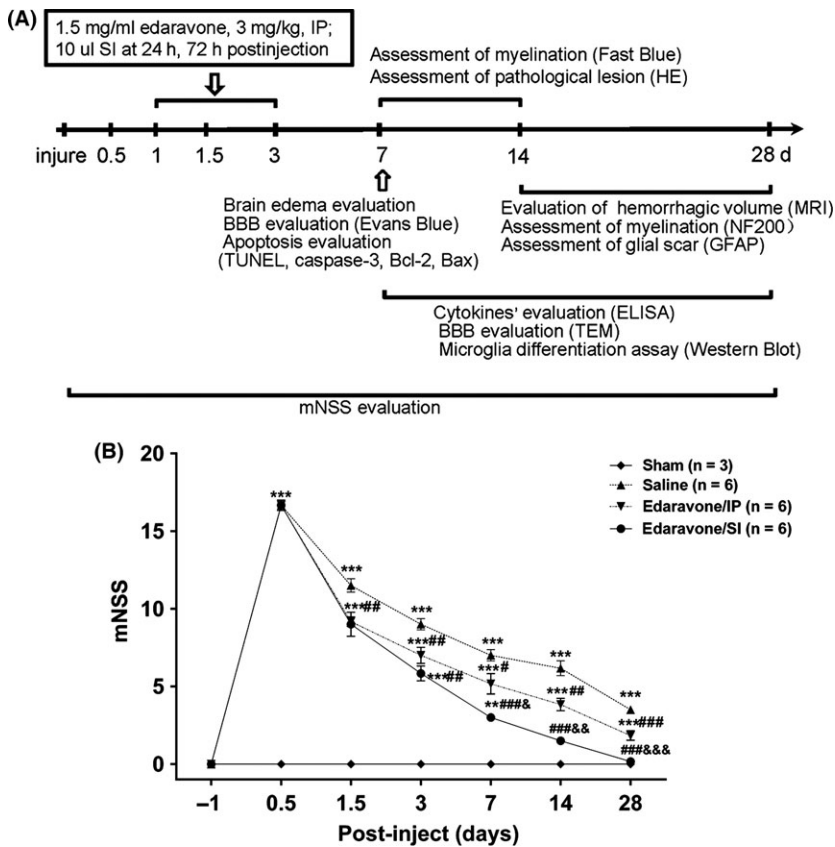
Figure 1 The schedule of experiment and improved outcome from the stereotactic administration of edaravone versus systemic route. (**A**) The intracerebral hemorrhage (ICH) was induced by collagenase VII, which is set the begin time (day 0) of all experiments. The chart illustrates the time of edaravone injection and all assays' schedule. (**B**) Modified neurological severity scores (mNSS) were examined at 1 day before ICH and days 0.5, 1.5, 3, 7, 14 and 28 post-inject. A significant improvement from day 7 to day 28 post-inject in the SI group compared with in the IP group. $*P < 0.05, **P < 0.01, ***P < 0.001$ versus the sham group; $^{\#}P < 0.05$, $^{\#\#}P < 0.01$, $^{\#\#\#}P < 0.001$ versus the saline group; $^{\&}P < 0.05$, $^{\&\&}P < 0.01$, $^{\&\&\&}P < 0.001$ versus the IP group.

protein (GFAP) (Cat#.ab7260, Abcam) for astrocytes; CD11b (Cat#.ab8878, Abcam) for microglia; arginase-1 (Cat#.ab91279, Abcam) for M2 marker; and iNOS (Cat#.ab4999, Abcam). To analyze apoptosis, three antibodies were used: Bax (Cat#. ab7977, Abcam), Bcl-2 (Cat#.ab136285, Abcam) and caspase-3 (Cat#.c8487, Sigma). Secondary antibodies were conjugated with Alexa Flour 488/555 (Invitrogen, Waltham, MA, USA).

Apoptotic cells and dying cells were assessed using terminal deoxyribonucleotidyltransferase-mediated d-Uridine 5′ triphosphate nick end labeling (TUNEL) according to the manufacturer's instructions (*In situ* cell death detection kit, AP; Roche Applied Science, Mannheim, Germany).

ELISA

TNF-α, IL-1β, IL-4, and IL-10 levels in brain tissues were determined with ELISA kit (Cloud-clone Group, Houston, TX, USA) at days 7, 14, and 28 post-ICH. During quantification, the cytokines were normalized to 100 μg of protein in the supernatant in accordance with the manufacturer's instructions.

Western Blot for Microglial Differentiation Assay

Brain tissues were lysed immediately to semiquantitatively analyze iNOS and arginase-1 expression by Western blot according to our previous studies [11].

Statistical Analysis

Data were expressed as mean ± standard error mean (SEM). Differences between groups were analyzed using one-way factorial analysis of variance (ANOVA). The general linear model was used for repeated measures. The Bonferroni correction was used to correct multiple comparisons. In all instances, n refers to the number of rats. A $P < 0.05$ was considered statistically significant (two-sided test, $\alpha = 0.05$). All statistics were calculated using SPSS 21.0 (SPSS Inc., Chicago, IL, USA), and plots were drawn using prism 6.0 software.

Results

Stereotactic Injection of Edaravone Improved Neurological Defects

In the sham group, the mNSS scores were zero at all time points. Conversely, the mNSS scores in the remaining three groups peaked at 12 h post-ICH and then gradually decreased over time (shown in Figure 1B). At day 7, the difference between the SI and IP groups was significant ($P = 0.014$) and became more significant with time.

Histopathological changes were analyzed by H&E staining in tissue sections of rats from the saline, IP, and SI groups (Figure 2A). At 7 days post-ICH, the SI group had slightly smaller hemorrhagic
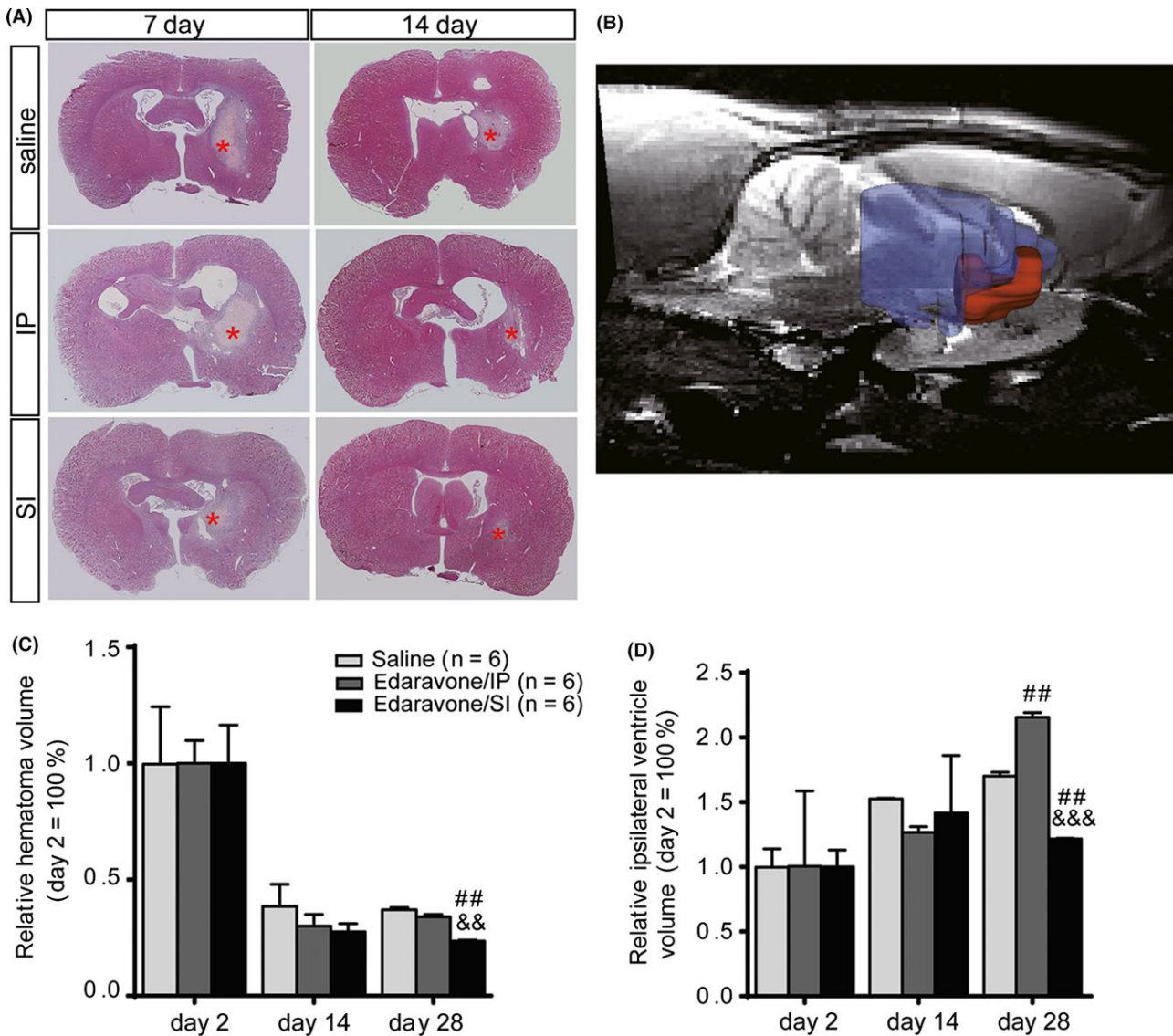
Figure 2 Evidence for improvement in intracerebral hemorrhage (ICH) treatment studied by histological changes and brain MRI. (**A**) H&E staining of brain tissue shows the hemorrhagic region and morphological changes. (**B**) Schematic diagram of hematoma volume was assessed by whole-brain MRI. Hematoma volume (red area) and ipsilateral ventricle volume (blue area) were observed via T2 times. (**C**) The relative hematoma volume at days 14 and 28 to day 2 post-ICH per treatment group was assessed by MRI. (**D**) The relative ipsilateral ventricular volume at days 14 and 28 to day 2 post-ICH per treatment group was assessed by MRI. $^{\#}P < 0.05$, $^{\#\#}P < 0.01$, $^{\#\#\#}P < 0.001$ versus the saline group; $^{\&}P < 0.05$, $^{\&\&}P < 0.01$, $^{\&\&\&}P < 0.001$ versus the IP group. Red stars indicate hematoma regions.

foci with relatively milder edema in the adjacent brain tissue compared with the other two groups. At day 14, the hemorrhagic foci were markedly decreased and brain edema was alleviated.

Hematoma volume was not significantly different between the three groups (saline, SI, and IP) at days 2 and 14 post-ICH according to MRI scan results. However, by day 28 post-ICH, the ratio of hematoma volume in the SI group was significantly smaller than in the saline ($P = 0.003$) and IP groups ($P = 0.007$) (Figure 2B,C). Additionally, the SI group had a significantly smaller ratio of ipsilateral ventricle volume than that of the saline ($P = 0.004$) and IP groups ($P < 0.001$) (Figure 2B,D). Original MRI images are shown in Figure S1.

We then analyzed cerebral edema based on water content. At day 7 (peak of cerebral edema), the wet/dry weight ratio (W/D) of the brain revealed significant differences between the four groups ($P < 0.001$). Bonferroni-corrected multiple tests implicated that both the IP and SI groups had significantly lower W/D than the saline group ($P < 0.01$), but higher than the sham group ($P < 0.01$). Most importantly, the W/D was significantly lower in the SI group than in the IP group ($P = 0.043$, Figure 3A).

Evans blue dye concentration in the brain tissue can be used to reflect BBB damage. As shown in Figure 3B, BBB damage was most severe in the saline group, but relatively mild in the IP and
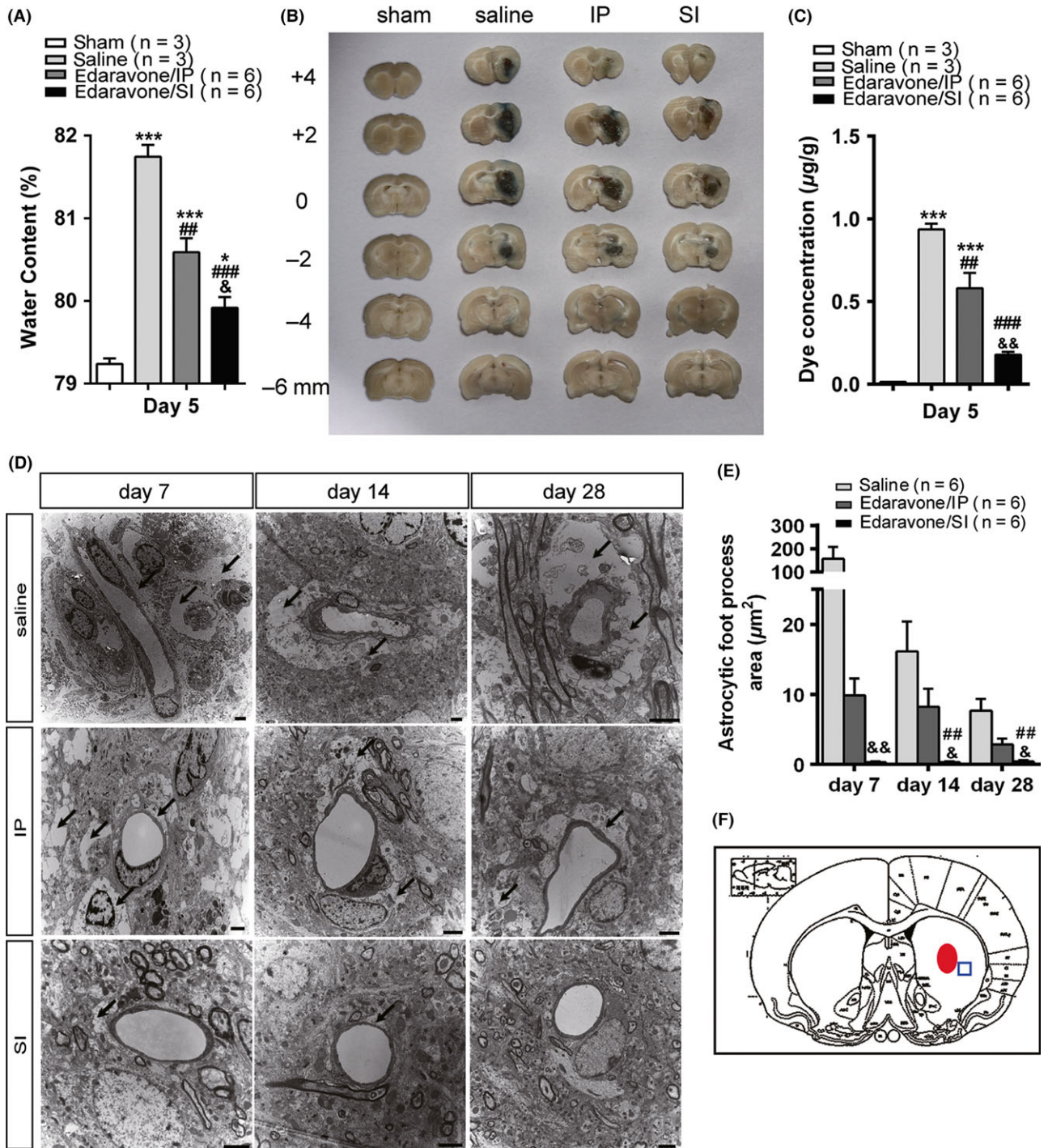
Figure 3 Evaluation of the brain edema and the vascular permeability of blood–brain barrier. (**A**) Brain water content evaluated at day 5 post-intracerebral hemorrhage (ICH). The water content of brain tissue = [(wet weight) − (dry weight)]/(wet weight) × 100%. (**B**) Representative brain coronal sections (2 mm thickness) show Evans blue extravasation at day 5 post-ICH. (**C**) Comparisons of dye concentrations among sham, saline, IP, and SI groups. The dye concentration is indicated as μg/g of tissue weight and calculated from a standard curve. (**D**) The brain tissues in penumbra around the hematoma post-ICH were sampled for transmission electron microscope. (**E**) Astrocyte foot process in edema area is significantly lower in SI than in the IP group. (**F**) Images were sampled from the brain tissue around the focus of cerebral hemorrhage. $^*P < 0.05, ^{**}P < 0.01, ^{***}P < 0.001$ versus the sham group; $^{\#}P < 0.05, ^{\#\#}P < 0.01, ^{\#\#\#}P < 0.001$ versus the saline group; $^{\&}P < 0.05, ^{\&\&}P < 0.01, ^{\&\&\&}P < 0.001$ versus the IP group. Black arrows indicate hematoma.

SI groups at day 7 post-ICH. The difference was significant between the SI and IP groups ($P = 0.003$, Figure 3C).

Electron microscopy results (Figure 3D) showed that the edema degree in astrocyte foot processes was significantly different between the three groups at four observation points ($P < 0.001$). The degree of edema in the SI group was significantly lower than in the IP group ($P = 0.003$) and gradually returned to normal over time (Figure 3E).

Stereotactic Injection of Edaravone Improved Neuropathology

At 7 days post-ICH, the ratio of the myelin sheath area in injured side to that in contralateral side decreased significantly in the SI group ($P = 0.041$). By day 14, ratios of myelin sheath area in the SI and IP groups were significantly lower than in the saline group ($P < 0.05$). Moreover, the SI group had a greater ratio of myelin sheath area compared with the IP group ($P = 0.046$) (Figure 4A,B).

Neurofilament protein, NF200, is an important component of the cytoskeleton and can directly reflect changes in neuronal axons. At day 14 post-ICH, NF200 expression significantly was enhanced in the SI group, but significantly decreased in the saline group (nearly disappeared). In the IP group, the intensity of neurofilaments slightly increased, and the neurofilaments were gathered into bundles. Compared with the saline group, there was no significant difference ($P = 0.999$). In contrast, the SI group had significantly higher NF200 expression than the saline group ($P < 0.001$) and the IP group ($P < 0.001$) (Figure 4C,D). At day 28 post-ICH, neurofilament expression had not returned to normal in the saline group and the IP group, and there was no significant difference between these two groups ($P = 0.609$). In the SI group, the neurofilaments were gathered into a network structure. Compared with the saline group ($P < 0.001$) and the IP group ($P < 0.001$), neurofilament distribution in the SI group was normal, although NF200 expression was significantly increased.

At day 14 post-ICH, the glial filaments, which were labeled by GFAP, were larger and thicker and were more densely distributed (Figure 4E). In the IP and SI groups, GFAP expression was significantly decreased respectively compared with the saline group ($P < 0.001$), but there was no difference between the SI and IP groups ($P = 0.936$). At day 28, the glial cells were irregularly enlarged and arranged in disorderly fashion with shorter cell protrusions. The glial reaction was markedly downregulated in the IP group. However, in the SI group, the morphology, cell number, protrusion amount, arrangement of glial cells, and GFAP expression level were nearly normal. Moreover, the improved glial reaction in the SI group was significantly greater to that in the IP group ($P = 0.013$) (Figure 4F).

Stereotactic Injection of Edaravone Promoted Microglia Cells to Differentiate into M2-Type Antiinflammatory Cells and Inhibited Differentiation into Pro-inflammatory M1 Type Cells

Arginase-1 (Arg1) is a marker for M2 microglia cells. The Arg1/CD11b ratio can reveal the polarization degree of M2 microglia.

On day 7 postsurgery, the ratio in the SI group was significantly different from the saline group ($P < 0.001$) and the IP group ($P < 0.001$) after Bonferroni correction. At day 14, the differences were still significant (Figure 5A,C). Western blotting also suggested that Arg1 expression in the saline group was significantly less than in the IP ($P = 0.006$) and SI groups ($P < 0.001$) at day 7 post-ICH. Additionally, the SI group was superior to the IP group with regard to promoting M2 microglial differentiation ($P = 0.043$) (Figure 5E,F).

iNOS is a marker for M1-type microglia. The iNOS/CD11b ratio can reveal the polarization degree of M1 microglia. On day 7 post-ICH, the ratios were 0.328 ± 0.028, 0.211 ± 0.007, and 0.055 ± 0.005 in the saline, IP, and SI groups, respectively. On day 14 post-ICH, the rations were 0.219 ± 0.001, 0.112 ± 0.010, and 0.030 ± 0.004, respectively. Bonferroni-corrected multiple tests showed that the iNOS/CD11b ratio was significantly different between groups on days 7 and 14 post-ICH ($P < 0.001$) (Figure 5B,D). Western blotting also suggested that the ratio in the saline group was significantly higher on day 7 post-ICH than in the IP group ($P = 0.005$) and the SI group ($P < 0.001$) (Figure 5E, G).

Stereotactic Injection of Edaravone Promoted Expression of Pro-Inflammatory Cytokines and Inhibited Expression of AntiInflammatory Cytokines

Expression of pro-inflammatory cytokines (IL-1β and TNF-α) and antiinflammatory cytokines (IL-4 and IL-10) was evaluated. IL-1β level decreased sequentially in the saline (3351.263 ± 475.618 pg/mg), IP (2472.324 ± 187.576 pg/mg), and SI groups (1655.143 ± 87.075 pg/mg) at day 7, respectively, with significant group differences ($P < 0.05$). At day 14, IL-1β expression in the SI group (318.000 ± 89.816 pg/mg) decreased significantly compared with that in the saline (1306.621 ± 316.319 pg/mg, $P = 0.012$) and IP groups (1140.510 ± 326.150 pg/mg, $P = 0.028$) (Figure 5H). Additionally, the level of IL-1β declined over time.

TNF-α expression was decreased significantly in the SI group (367.223 ± 47.730 pg/mg) than in the IP group (504.760 ± 32.929 pg/mg, $P = 0.022$) at day 14 (Figure 5I). IL-4 level (942.990 ± 178.284 and 1359.714 ± 229.906 pg/mg, respectively) at days 7 and 14 post-ICH was significantly increased compared with the IP group (630.036 ± 67.527 and 833.097 ± 75.941 pg/mg, respectively) (Figure 5J). IL-10 expression was significantly greater in the SI group than in the other two groups at all time points. Compared with the IP group, the IL-10 expression in the SI group was significantly higher at day 14 (601.333 ± 43.137 vs. 430.725 ± 27.124 pg/mg, $P = 0.002$). And the expression of IL-10 lasted up to day 28 post-ICH ($P = 0.030$) (Figure 5K).

Stereotactic Injection of Edaravone Inhibited Neural Cell Apoptosis Following ICH

At day 7 after ICH, the number of TUNEL-positive cells decreased sequentially in the saline, IP, and SI groups, with 52.666 ± 4.041, 33.333 ± 3.511 and 16.333 ± 5.686 TUNEL-positive cells per
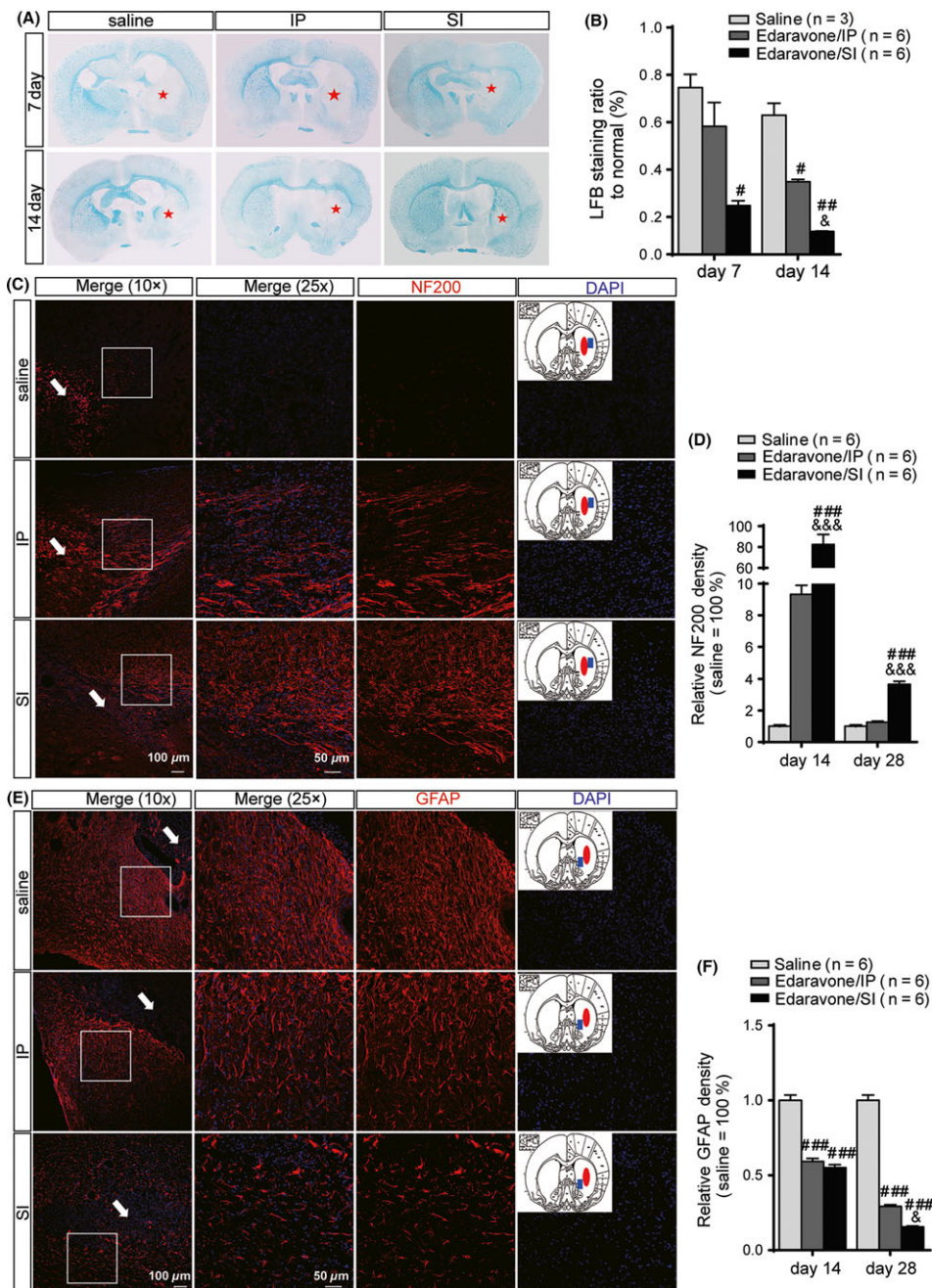
Figure 4 Evaluation of neuropathology in axon, astrocyte activation, and myelination. (**A**) Representative brain coronal sections (2 mm thickness) show the degree of myelination by Luxol fast blue(LFB) staining. (**B**) The LFB staining ratio to normal is significantly lower in SI than the saline group at both days 7 and 14 post-intracerebral hemorrhage (ICH) and the IP group on day 14 post-ICH. (**C**) Molecular marker NF200 (red fluorescence) was used to assess neuropathology improvement in axon by immunostaining. Anatomy diagram of rat brain in each treatment group shows the hemorrhagic foci (red solid ellipse) and sampling location (blue solid square). Merged images (25×) are sampled from the white square in the corresponding low magnification images (10×), where the white arrows indicate the hemorrhagic foci.(**D**) The expression of NF200 in SI increased significantly higher than that in the saline and IP groups. (**E**) Molecular marker glial fibrillary acidic protein (GFAP) (red fluorescence) was used to assess astrocyte activation by immunostaining. Anatomy diagram of rat brain in each treatment group shows the hemorrhagic foci (red solid ellipse) and sampling location (blue solid square). Merged images (25×) are sampled from the white square in the corresponding low magnification images (10×), where the white arrows indicate the hemorrhagic foci.(**F**) The expression of GFAP decreased significantly in SI and IP than in the saline group. Both the density values of LFB staining and the fluorescence intensity values were calculated by Image-Pro Plus 6.0. $^{\#}P < 0.05$, $^{\#\#}P < 0.01$, $^{\#\#\#}P < 0.001$ versus the saline group; $^{\&}P < 0.05$, $^{\&\&}P < 0.01$, $^{\&\&\&}P < 0.001$ versus the IP group. Red stars indicate myelin sheath damage region.
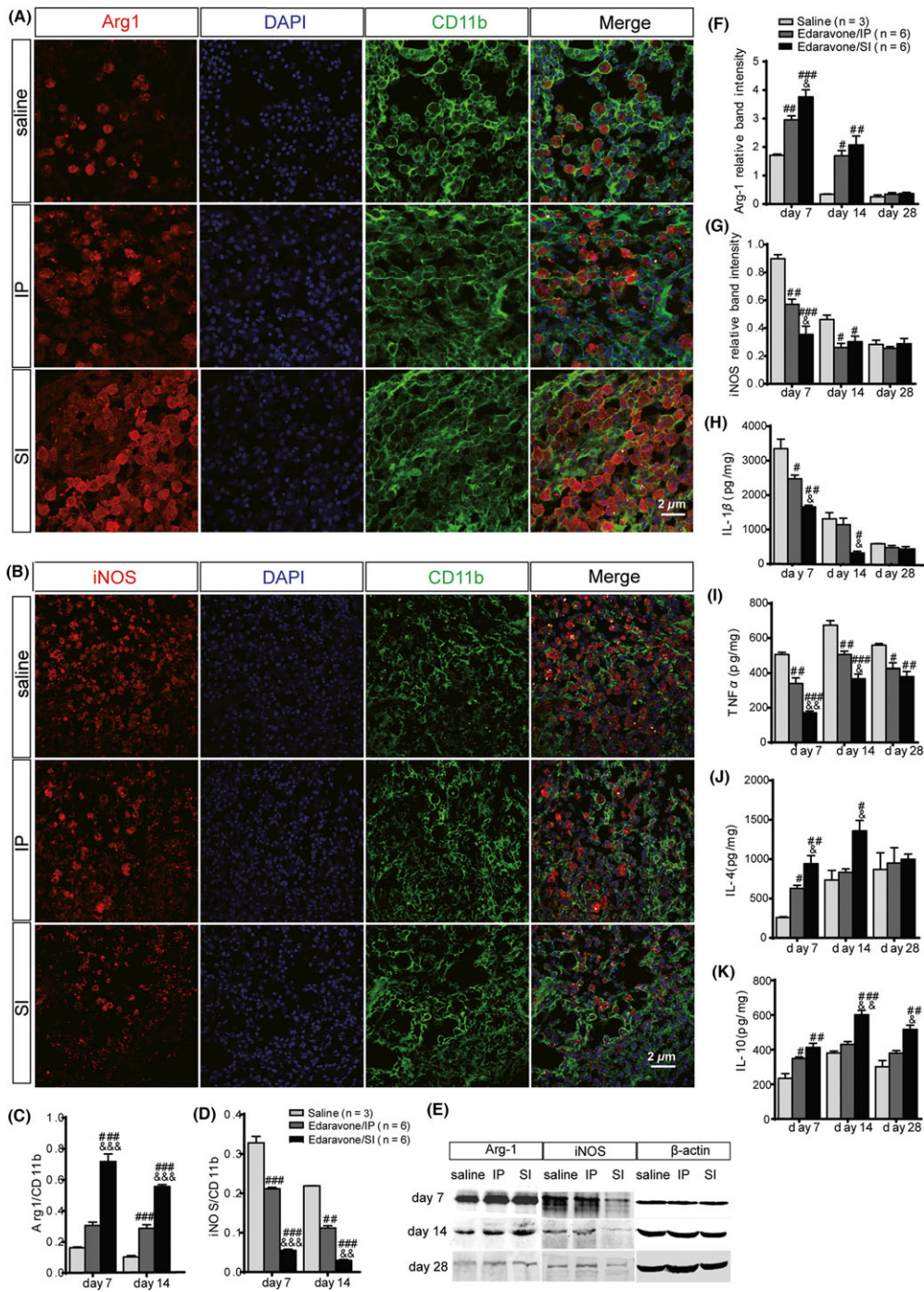
Figure 5 Assessment of microglia differentiation and cytokines' levels in rat brain tissues. Microglia differentiation was observed by immunofluorescent staining. Arginase-1 (**A**) (red) is a marker of M2 microglia. iNOS (**B**) (red) is a marker of M1 microglia. CD11b (green) is another epitope for microglia. The Arginase-1/CD11b (**C**) revealed the polarization degree of M2 microglia. In the SI group, microglia differentiated higher markedly into type M2 than that in the saline and IP groups. The iNOS/CD11b (**D**) revealed the polarization degree of M1 microglia. The polarization degree of M1 microglia in SI was inhibited more dramatically than that in the saline and IP groups at days 7 and 14 post-intracerebral hemorrhage. (**E**) Microglia differentiation was evaluated by iNOS and arginase-1 semiquantitative analysis using Western blot. Arginase-1 (**F**) level increased significantly in SI than in the IP group at days 7 and 14 post-operation. On the contrary, iNOS (**G**) level decreased significantly. The relative band intensity was normalized to the level of β-actin. The level of a serial inflammantory and anti-inflammantory molecules, IL-1β (**H**), TNF-α (**I**), and IL-4 (**J**) as well as IL-10 (**K**) were studied by ELISA. $^{#}P < 0.05$, $^{##}P < 0.01$, $^{###}P < 0.001$ versus the saline group; $^{&}P < 0.05$, $^{&&}P < 0.01$, $^{&&&}P < 0.001$ versus the IP group.
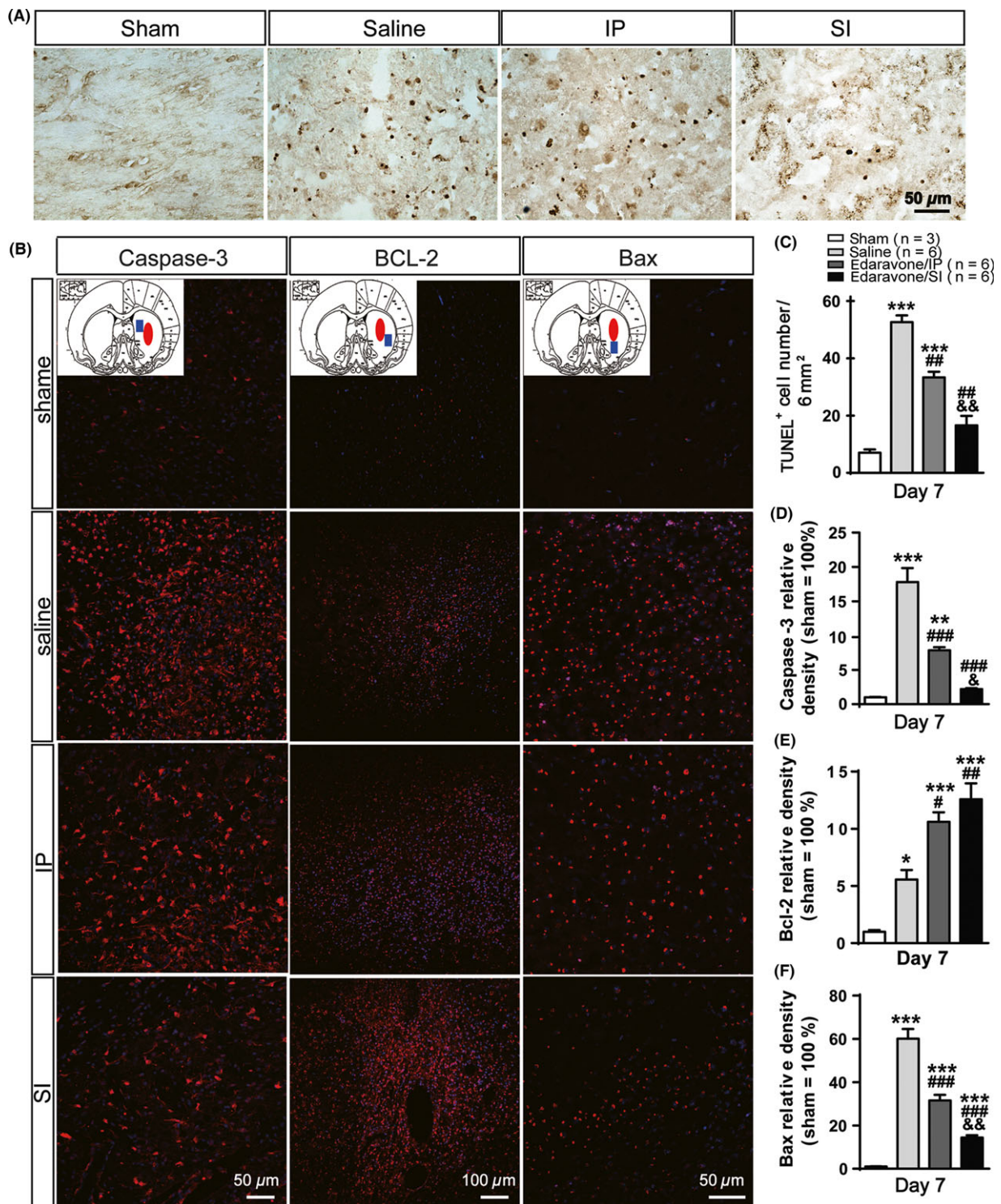
Figure 6 The detection of dying cells and apoptosis-related proteinsat day 7 post-intracerebral hemorrhage (ICH). (**A**) Detection of apoptosis by the TUNEL assay. Typical apoptotic morphology is indicated in brown. (**B**) The levels of apoptosis-related proteins, caspase-3, Bcl-2 and Bax, in brain tissues were assessed by the fluorescent confocal microscopy. Anatomy diagram of rat brain at each gene column shows the sampling location (blue solid square) relative to the hemorrhagic foci (red solid ellipse) (**C**) ICH-induced neural cellsapoptosis. Edaravone could inhibit significantly the process of apoptosis in SI compared with the IP group. Caspase-3 (**D**) and Bax (**F**) both have lower expression in the SI group than in the IP group. And the expression of Bcl-2 increased more obviously in SI than in other groups (**E**). *$P < 0.05$,**$P < 0.01$,***$P < 0.001$ versus the sham group; #$P < 0.05$, ##$P < 0.01$, ###$P < 0.001$ versus the saline group; &$P < 0.05$, &&$P < 0.01$, &&&$P < 0.001$ versus the IP group.

visual field, respectively (Figure 6A,C). The number of apoptotic cells was significantly different between groups (except between the SI group and the sham group) ($P < 0.05$). Immunofluorescence detection of apoptosis proteins showed that edaravone inhibited relative expression of the pro-apoptotic gene *Caspase-3*. Additionally, the treatment efficacy was superior in the SI group compared with in the IP group ($P = 0.026$). Significant differences existed between the four groups (except between the SI and sham groups) ($P < 0.05$) (Figure 6B,D). The changes in antiapoptotic gene *Bcl-2* expression showed a reverse trend in relative expression, which increased respectively in the sham (1.000 ± 0.251), saline (5.559 ± 1.459), IP (10.615 ± 1.432), and SI groups (12.582 ± 2.407). The difference was significant between the four groups ($P < 0.05$), except between the SI and the IP groups ($P = 1.000$) (Figure 6B,E). Finally, compared with the sham group, expression of the apoptotic gene *Bax* was gradually decreased in the saline (60.081 ± 7.870), IP (31.565 ± 4.519), and SI groups (14.394 ± 1.885). There was a significant difference between any two groups ($P < 0.05$) (Figure 6B,F).

Discussion

Edaravone has been widely used in China, and results have suggested that it may be beneficial in acute ICH [13]. It is possible, however, that different routes of administration could affect the treatment efficacy. This study was the first to demonstrate intracranial stereotactic injection of edaravone in an ICH rat model. We also confirmed the significant neuroprotective effect of edaravone on ICH through the combination of histopathological and imaging studies.

We have compared drug effect between two administration routes of edaravone until day 28 after ICH. Majority of researchers have selected similar limited time points to study [7,14,15]. For example, Rosenberg [16] suggested that long-term histopathological protection should be examined at 28 days following collagenase-induced ICH. Power et al. [7] assessed functional protection up to 28 days after ICH. Chen et al. [14] observed morphological changes at day 28 postinjection in rats treated by edaravone. Rats with ICH basically returned to normal at day 28 post-ICH [16]; thus, any analysis after day 28 post-ICH has little clinical significance. Data collected up to 28 days already proves our hypothesis that the effect of stereotactic injection is better than intraperitoneal injection.

The edaravone dose for i.p. injection was based on relevant literature [17–19]. Watanabe et al. [19] reported that 3 mg/kg decreased the cerebral infarction size in adult rats. Other studies also used the same edaravone dose [17,18]. So, we chose this dose for our study. Dosing intervals reported in rats are diverse, such as 3 mg/kg (i.p.) once a day for 3 weeks [20], once a day for 7 days [21], a single dose [22], twice daily at days 1 and 5 [23], which depend on research objects. For maximizing therapeutic effects, our dosing intervals were dependent on the three therapeutic windows of brain edema, the hyperacute phase (≤ 3 h), the acute phase (≤ 24 h), and the subacute phase (72 h). Other studies reported that penumbra in humans can exist for a long period, at least up to 48 h [23] and even for several days [24]. Therefore, we initially treated rats at 1 h post-ICH, then once a day for 3 days.

According to our object, we pay more attention to the comparability of drug dose between two routes than the difference between several dosages of edaravone, although it is also meaningful. The SI dose and the IP dose are comparable. Namely, the concentration of 3 mg/kg in IP is equivalent to the concentration of 26 μg/mL (3 mg/kg $\times$ 0.265 kg $\times$ 0.8 $\div$ 14.6 mL $\times$ 0.6 =26 μg/mL) in the brain. In SI, 10 μL edaravone of 1.5 mg/mL was injected into the brain, and the concentration was also about 26 μg/mL (1.5 mg/mL $\times$ 10 μL $\div$ 580 μL = 26 μg/mL) in the hematoma loci.

To increase comparability, the dosing intervals of stereotactic injections were also dependent on the therapeutic windows. Cerebral hemorrhage induced by collagenase is not stable during the hyperacute phase (≤ 3 h). Therefore, edaravone should not be administered at 1 h postinjection. To better simulate the clinical situation, we initially administered edaravone at 24 h post-ICH. Because the curative effect of edaravone is independent of the treatment time interval (i.e., ≤ 24, 25–48 or 48–72 h) [25] to reduce brain damage caused by repeated injections and to maximize the curative effect through prolonging action period, we elongated time without administering any drug at 48 h after ICH. The last time to delivery edaravone was at 72 h post-ICH, which was the subacute phase onset of ICH. We did test kinetics and dynamics of edaravone in the brain tissue by the both administrations and found that the half-life of edaravone in cerebral spinal fluid by SI was longer than that by IP in our preliminary experiments. In fact, results based on two treatment points at 24 and 72 h post-ICH showed that the curative effect by stereotactic administration was better than by intraperitoneal injection.

It is interesting that the mNSS decreased as early as 1.5 day postinjury without changing the hematoma size and ipsilateral ventricle volume. Neurological functional change and tissue morphology change do not synchronize, and the former is more sensitivity and earlier than the latter. More pertinent to the present results is a study [7] in which neurobehavioral performance improved at day 1 after ICH in treatment group than control group, while there is no difference in the size of the lesion between two groups; that is, the function change in neuron might be caused by cell damage, while the change in tissue morphology level cannot be observed. Moreover, edaravone can eliminate free radical released in the hyperacute (≤ 3 h) and the acute phase (≤ 24 h) of ICH, which improved the mNSS. These account partly for that mNSS significantly decreased on day 1.5, but MRI cannot detect the change in the hematoma size and ipsilateral ventricle volume. It postulated that earlier improvement in function may occur at cellular level.

The mNSS is the most important indicator of ICH treatment [26]. Results from the present study showed that the stereotactic route of edaravone administration yielded significantly better outcomes than the IP route in terms of lower mNSS scores, which was consistent with the report that edaravone improved neurological functions [5,9,14,27,28]. ICH damages the BBB, driving blood into the brain tissue, which results in cerebral edema [29]. Histopathological evidence from H&E staining, Evans blue staining, TEM observation, and brain tissue D/W ratio demonstrated that SI resulted in significant improvement over time compared with the other treatment paradigms.

Results from the immunohistochemical studies showed that NF200 expression was significantly greater in the SI group than in

the IP group. The SI group had an increased number of neurofilaments, which were tightly packed and gathered into a bundle. Additionally, GFAP expression was downregulated. Over time, GFAP expression in the SI group was significantly less than that in the IP group. Previous works have shown that excessive numbers of astrocytes can inhibit axonal regeneration [30,31]. Our results indicated that SI was more effective at reducing glial scar formation, which could further improve neurological function. This was consistent with the morphological observations already mentioned.

The therapeutic mechanisms of edaravone were also investigated in terms of antiinflammatory and antiapoptosis regulation. The pro-inflammatory cytokine TNF-α can increase BBB permeability, thereby worsening cerebral edema [32]. Several molecular pathways are involved in promotion of inflammation, thrombosis, and neurotoxic synthetic substances, as well as activation of the body's coagulation and fibrinolysis system [33–35]. We found that during the early stage of injury, compared with the IP group, stereotactic injection of edaravone significantly reduced TNF-α expression in the brain tissue. Edaravone could reduce TNF-α expression in ischemia and reperfusion-induced myocardial injury [36], as well as ischemic injury in rat microglia [37], which is consistent with the present results. We found that during the initial stage of ICH, IL-1β level was significantly less in the SI group than in the IP group, which was more effective at controlling inflammation and improving brain function. This effect was previously verified by injecting IL-1β into the rat brain, showing induction of transient inflammation and apoptosis. Patients with increased IL-1 suffered greater severity of the condition [38]. In addition, we found gradually increased expression of two inhibiting inflammatory cytokines (IL-4 and IL-10) over time. Compared with the IP group, stereotactic injection may promote secretion of IL-4 and IL-10 significantly. IL-4 exerts its antiinflammatory effects through many pathways [39], such as induction of M2 macrophage differentiation, secretion of cytokines including IL-10 and IL-12, and inhibition of free radical release. IL-10 can also induce M2 macrophage differentiation, regulate the immune system, and promote matrix deposition to repair brain tissue [39]. The inhibition of early inflammation could reduce the extent of early brain edema and brain tissue damage [40,41]. Hence, the occurrence of brain edema is inseparable from inflammation [42].

Microglia are immune effector cells of the central nervous system and can be characterized into the pro-inflammatory M1-type and antiinflammatory M2 type [43]. Compared with the IP group, expression of iNOS, an M1-type marker, was significantly reduced, and expression of arginase-1, an M2-type marker, was significantly increased in the SI group, as shown by immunofluorescence staining and Western blot assay. Therefore, stereotactic administration inhibits M1-type and promotes M2-type macrophage differentiation. The M1-type macrophages can produce large amounts of NO, a product of oxidative stress, and pro-inflammatory cytokines, which can cause damage to normal neurons and glial cells. Conversely, type M2 macrophages inhibit inflammation and promote angiogenesis and tissue repair [39]. Edaravone effection on macrophages was consistent with reduced expression of inflammatory cytokines, resulting in a combined effect of inhibiting inflammation, relieving brain edema and improving neurological function. Inflammation can lead to brain tissue damage [44], and damaged brain tissue releases large amounts of inflammatory cytokines, which in turn further aggravates the inflammatory reaction. A malignant cycle is formed, which eventually worsens the brain tissue damage and intensifies the edema, along with neurobehavioral disorders. Therefore, inflammation plays an important role in secondary brain injury in ICH.

A large number of apoptotic cells abounded in the hemorrhagic lesions and surrounding tissues of ICH rats, dominated by neurons and glial cells [45]. TUNEL assay revealed that SI significantly inhibited dying cells and apoptosis of neural cells within the hematoma tissue. Meanwhile, edaravone significantly inhibited *caspase-3* and *Bax* expression and increased *Bcl-2* expression, which was consistent with a previous report [46].

Compared with the intraperitoneal route of administration, stereotactic delivery achieved better efficacy. SI directly delivered edaravone into the hematoma region and bypassed the BBB, allowing the drug to be quickly absorbed by the brain tissue and to quickly reach therapeutic concentrations without missing the optimal period for ICH treatment. Indeed, we found that the half-life of edaravone in cerebral spinal fluid by SI was longer than that by IP (data not showed here). Additionally, a direct-targeted injection avoided a prolonged long distance course for drugs via the blood, which significantly reduced the side effects of edaravone. Nevertheless, topical administration requires professional stereotactic instrument, which is associated with certain invasiveness. These shortcomings could be minimized by the development of relevant technologies and procedures. With the wider application of automatic syringe pumps, stereotactic surgical procedures have been increasingly utilized. For patients with minor intracranial bleeding, requiring stereotactic minimally invasive surgery or local administration for conservative therapy, SI is the preferred approach. Our study has provided a theoretical basis for this rationale, and the stereotactic approach could help to reduce drug cost and avoid the excessive use of resources.

This study had some limitations. First, it was carried out in small animals, which made it impossible to treating lesions after removal of hematoma and affected the dose of edaravone in the hematoma cavity. Larger animals should be used in future studies to confirm the protective effect of different concentrations of edaravone for brain edema after hematoma removal. Second, we only studied the mechanisms involved in tissue inflammation and apoptosis. In future studies, other aspects (scavenging free radicals, protecting vascular endothelial cells, inhibition of vascular spasm, etc.) should be investigated.

In summary, stereotactic injection of edaravone is more effective for targeting hemorrhagic lesions, because it inhibits pro-inflammatory response and promotes the antiinflammatory response. It also inhibits neuronal apoptosis, reduces the extent of damage to BBB, reduces cerebral edema, and restores neuronal functions. Our study is the first to demonstrate the important advantage of intracranial stereotactic injection over systemic administration, which decreases the edaravone consumption and adverse effects and provides a potential option for the clinical treatment of ICH.

Acknowledgment

Conflict of Interest

The authors declare no conflict of interest.

References

1. McGuire AJ, Raikou M, Whittle I, Christensen MC. Long-term mortality, morbidity and hospital care following intracerebral hemorrhage: an 11-year cohort study. *Cerebrovasc Dis* 2007;**23**:221–228.

2. Enatsu R, Asahi M, Matsumoto M, Hirai O. Prognostic factors of motor recovery after stereotactic evacuation of intracerebral hematoma. *Tohoku J Exp Med* 2012;**227**:63–67.

3. Thiex R. Future perspectives on the fibrinolytic therapy of intracerebral hemorrhages. *Cent Nerv Syst Agents Med Chem* 2011;**11**:150–156.

4. Roth C, Kastner S, Salehi M, Kleffmann J, Boker DK, Deinsberger W. Comparison of spontaneous intracerebral hemorrhage treatment in Germany between 1999 and 2009: results of a survey. *Stroke* 2012;**43**:3212–3217.

5. Shang H, Cui D, Yang D, Liang S, Zhang W, Zhao W. The radical scavenger edaravone improves neurologic function and perihematomal glucose metabolism after acute intracerebral hemorrhage. *J Stroke Cerebrovasc Dis* 2015;**24**:215–222.

6. Rennert RC, Signorelli JW, Abraham P, Pannell JS, Khalessi AA. Minimally invasive treatment of intracerebral hemorrhage. *Expert Rev Neurother* 2015;**15**:919–933.

7. Power C, Henry S, Del BM, et al. Intracerebral hemorrhage induces macrophage activation and matrix metalloproteinases. *Ann Neurol* 2003;**53**:731–742.

8. Bao X, Wei J, Feng M, et al. Transplantation of human bone marrow-derived mesenchymal stem cells promotes behavioral recovery and endogenous neurogenesis after cerebral ischemia in rats. *Brain Res* 2011;**1367**:103–113.

9. Zhou F, Chen G, Zhang J. Edaravone reduces brain oedema and attenuates cell death after intracerebral haemorrhage in mice. *Brain Inj* 2009;**23**:353–357.

10. Liew HK, Pang CY, Hsu CW, et al. Systemic administration of urocortin after intracerebral hemorrhage reduces neurological deficits and neuroinflammation in rats. *J Neuroinflammation* 2012;**9**:13.

11. Zhang MY, Zheng CY, Zou MM, et al. Lamotrigine attenuates deficits in synaptic plasticity and accumulation of amyloid plaques in APP/PS1 transgenic mice. *Neurobiol Aging* 2014;**35**:2713–2725.

12. Yang Y, Zhang Y, Wang Z, et al. Attenuation of Acute Phase Injury in Rat Intracranial Hemorrhage by Cerebrolysin that Inhibits Brain Edema and Inflammatory Response. *Neurochem Res* 2015;**41**:1–10.

13. Yang J, Liu M, Zhou J, Zhang S, Lin S, Zhao H. Edaravone for acute intracerebral haemorrhage. *Cochrane Database Syst Rev*. DOI: 10.1002/14651858.CD007755.pub2

14. Chen D, Liu Y, Zhu J, Wang S. Experimental study of edaravone on neuroprotective effect in intracerebral hemorrhage of rats [J]. *China J Mod Med* 2009;**4**:7.

15. Szymanska A, Biernaskie J, Laidley D, Granter-Button S, Corbett D. Minocycline and intracerebral hemorrhage: influence of injury severity and delay to treatment. *Exp Neurol* 2006;**197**:189–196.

16. Rosenberg GA, Mun-Bryce S, Wesley M, Kornfeld M. Collagenase-induced intracerebral hemorrhage in rats. *Stroke* 1990;**21**:801–807.

17. Song Y, Gong YY, Xie ZG, Li CH, Gu Q, Wu XW. Edaravone (MCI-186), a free radical scavenger, attenuates retinal ischemia/reperfusion injury in rats. *Acta Pharmacol Sin* 2008;**29**:823–828.

18. Sun YY, Morozov YM, Yang D, et al. Synergy of combined tPA-edaravone therapy in experimental thrombotic stroke. *PLoS One* 2014;**9**:e98807.

19. Watanabe T, Yuki S, Egawa M, Nishi H. Protective effects of MCI-186 on cerebral ischemia: possible involvement of free radical scavenging and antioxidant actions. *J Pharmacol Exp Ther* 1994;**268**:1597–1604.

20. Nimata M, Okabe TA, Hattori M, Yuan Z, Shioji K, Kishimoto C. MCI-186 (edaravone), a novel free radical scavenger, protects against acute autoimmune myocarditis in rats. *Am J Physiol Heart Circ Physiol* 2005;**289**:H2514–H2518.

21. Horiike O, Shimogori H, Ikeda T, Yamashita H. Protective effect of edaravone against streptomycin-induced vestibulotoxicity in the guinea pig. *Eur J Pharmacol* 2003;**464**:75–78.

22. Kamida T, Fujiki M, Ooba H, Anan M, Abe T, Kobayashi H. Neuroprotective effects of edaravone, a free radical scavenger, on the rat hippocampus after pilocarpine-induced status epilepticus. *Seizure* 2009;**18**:71–75.

23. Heiss WD, Huber M, Fink GR, et al. Progressive derangement of periinfarct viable tissue in ischemic stroke. *J Cereb Blood Flow Metab* 1992;**12**:193–203.

24. Saunders DE, Howe FA, van den Boogaart A, McLean MA, Griffiths JR, Brown MM. Continuing ischemic damage after acute middle cerebral artery infarction in humans demonstrated by short-echo proton spectroscopy. *Stroke* 1995;**26**:1007–1013.

25. Lapchak PA. A critical assessment of edaravone acute ischemic stroke efficacy trials: is edaravone an effective neuroprotective therapy? *Expert Opin Pharmacother* 2010;**11**:1753–1763.

26. Lu M, Chen J, Lu D, Yi L, Mahmood A, Chopp M. Global test statistics for treatment effect of stroke and traumatic brain injury in rats with administration of bone marrow stromal cells. *J Neurosci Methods* 2003;**128**:183–190.

27. Nakamura T, Kuroda Y, Yamashita S, et al. Edaravone attenuates brain edema and neurologic deficits in a rat model of acute intracerebral hemorrhage. *Stroke* 2008;**39**:463–469.

28. Yagi K, Kitazato KT, Uno M, et al. Edaravone, a free radical scavenger, inhibits MMP-9-related brain hemorrhage in rats treated with tissue plasminogen activator. *Stroke* 2009;**40**:626–631.

29. Bai J, Lyden PD. Revisiting cerebral postischemic reperfusion injury: new insights in understanding reperfusion failure, hemorrhage, and edema. *Int J Stroke* 2015;**10**:143–152.

30. Xiong M, Yang Y, Chen GQ, Zhou WH. Post-ischemic hypothermia for 24 h in P7 rats rescues hippocampal neuron: association with decreased astrocyte activation and inflammatory cytokine expression. *Brain Res Bull* 2009;**79**:351–357.

31. Sofroniew MV, Vinters HV. Astrocytes: biology and pathology. *Acta Neuropathol* 2010;**119**:7–35.

32. King MD, Alleyne CJ, Dhandapani KM. TNF-alpha receptor antagonist, R-7050, improves neurological outcomes following intracerebral hemorrhage in mice. *Neurosci Lett* 2013;**542**:92–96.

33. Tuttolomondo A, Pecoraro R, Pinto A. Studies of selective TNF inhibitors in the treatment of brain injury from stroke and trauma: a review of the evidence to date. *Drug Des Devel Ther* 2014;**8**:2221–2238.

34. Doll DN, Rellick SL, Barr TL, Ren X, Simpkins JW. Rapid mitochondrial dysfunction mediates TNF-alpha-induced neurotoxicity. *J Neurochem* 2015;**132**:443–451.

35. McCoy MK, Tansey MG. TNF signaling inhibition in the CNS: implications for normal brain function and neurodegenerative disease. *J Neuroinflammation* 2008;**5**:45.

36. Onimaru S, Nakamura K, Kariyazono H, et al. Inhibitory effects of edaravone on the production of tumor necrosis factor-alpha in the isolated heart undergoing ischemia and reperfusion. *Heart Vessels* 2006;**21**:108–115.

37. Yuan Y, Zha H, Rangarajan P, Ling EA, Wu C. Anti-inflammatory effects of Edaravone and Scutellarin in activated microglia in experimentally induced ischemia injury in rats and in BV-2 microglia. *BMC Neurosci* 2014;**15**:125.

38. Holmin S, Mathiesen T. Intracerebral administration of interleukin-1beta and induction of inflammation, apoptosis, and vasogenic edema. *J Neurosurg* 2000;**92**:108–120.

39. Martinez FO, Gordon S. The M1 and M2 paradigm of macrophage activation: time for reassessment. *F1000Prime Rep.* 2014;**6**:13.

40. Zhang ZL, Liu YG, Huang QB, et al. Nuclear factor-kappaB activation in perihematomal brain tissue correlates with outcome in patients with intracerebral hemorrhage. *J Neuroinflammation* 2015;**12**:53.

41. Zhang XS, Zhang X, Wu Q, et al. Astaxanthin offers neuroprotection and reduces neuroinflammation in experimental subarachnoid hemorrhage. *J Surg Res* 2014;**192**:206–213.

42. Wasserman JK, Schlichter LC. Minocycline protects the blood-brain barrier and reduces edema following intracerebral hemorrhage in the rat. *Exp Neurol* 2007;**207**:227–237.

43. Tang Y, Le W. Differential Roles of M1 and M2 Microglia in Neurodegenerative Diseases. *Mol Neurobiol* 2016;**53**:1181–1194.

44. Ma JQ, Luo RZ, Jiang HX, Liu CM. Quercitrin offers protection against brain injury in mice by inhibiting oxidative stress and inflammation. *Food Funct* 2016;**7**:549–556.

45. Felberg RA, Grotta JC, Shirzadi AL, et al. Cell death in experimental intracerebral hemorrhage: the "black hole" model of hemorrhagic damage. *Ann Neurol* 2002;**51**:517–524.

46. Li JM, Zhang P, Zhao YN, Chen CX, Li SX. Protective effects of edaravone on diffuse brain injury in rats. *World J Emerg Med* 2011;**2**:222–227.

Supporting Information

The following supplementary material is available for this article:

Figure S1. Original images for improvement of ICH treatment studied by MRI.